

# NASA TECHNICAL MEMORANDUM

NASA TM X-52793

NASA TM X-52793

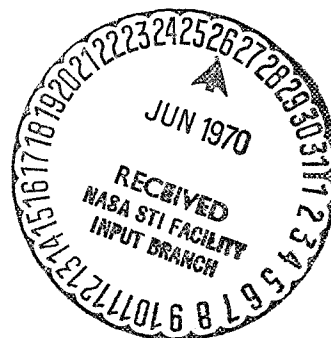
N70 25625

## CASE FILE COPY

APPLICATIONS OF VARIABLE PROPERTY HEAT-TRANSFER AND FRICTION  
EQUATIONS TO ROCKET NOZZLE COOLANT PASSAGES AND  
COMPARISON WITH NUCLEAR ROCKET TEST RESULTS

by Maynard F. Taylor  
Lewis Research Center  
Cleveland, Ohio

TECHNICAL PAPER proposed for presentation at  
Sixth Propulsion Joint Specialists Conference sponsored by the  
American Institute of Aeronautics and Astronautics  
San Diego, California, June 15-19, 1970



APPLICATIONS OF VARIABLE PROPERTY HEAT-TRANSFER AND FRICTION  
EQUATIONS TO ROCKET NOZZLE COOLANT PASSAGES AND  
COMPARISON WITH NUCLEAR ROCKET TEST RESULTS

by Maynard F. Taylor

Lewis Research Center  
Cleveland, Ohio

TECHNICAL PAPER proposed for presentation at  
Sixth Propulsion Joint Specialists Conference sponsored by  
the American Institute of Aeronautics and Astronautics  
San Diego, California, June 15-19, 1970

NATIONAL AERONAUTICS AND SPACE ADMINISTRATION

# APPLICATIONS OF VARIABLE PROPERTY HEAT-TRANSFER AND FRICTION EQUATIONS TO ROCKET NOZZLE COOLANT PASSAGES AND COMPARISON WITH NUCLEAR ROCKET TEST RESULTS

Maynard F. Taylor

Lewis Research Center  
National Aeronautics and Space Administration  
Cleveland, Ohio

## Abstract

The best available heat-transfer and friction correlations for single-phase turbulent flow of hydrogen through tubes with large ratios of wall to bulk temperatures are applied to the cooling passages of nuclear rocket nozzles. The calculated pressure drop and temperature rise of the coolant are compared to the measured values for nuclear test runs of Pewee, NERVA, and Phoebus 2A nozzles. Calculated local gas-side wall temperatures are compared with wall temperatures indicated by melting of selected braze alloys from NERVA nuclear tests. The use of several different heat-transfer correlations on the hot-gas side and their effect on the predicted wall temperature is also discussed.

## I. Introduction

An effective method of predicting heat-transfer and friction coefficients in the coolant passages of regeneratively cooled rocket nozzles is essential to the optimization of any nozzle design. In nuclear rocket nozzles the heat flux in the throat region can be of the order of 20 Btu/sec/in.<sup>2</sup>. A heat flux of as much as 100 Btu/sec/in.<sup>2</sup> are predicted as possible in advanced chemical rocket concepts.

The author of this paper has previously studied all available single-phase hydrogen heat-transfer data for flow through straight tubes and recommended a single correlation equation for a wide range of conditions.<sup>(1)</sup> The calculated heat-transfer coefficients were shown to be in very good agreement with the high heat flux experimental data.<sup>(2)</sup> The straight tube equation has been modified to include the effects of curvature<sup>(3)</sup> and compared with experimental data for single curved tubes.<sup>(2,4)</sup> These results and recommended applications of the equations have been reported.<sup>(5)</sup>

In addition all available experimental friction coefficients have been analyzed and a new correlation equation recommended for single-phase turbulent flow through smooth straight tubes.<sup>(6)</sup> The straight tube equation for friction can be modified to include the effects of curvature.<sup>(3)</sup>

In this paper the best available heat-transfer and friction correlation equations are brought together and applied to the cooling passages of nuclear rocket nozzles. The most severe test of the ability of these equations to calculate heat transfer and friction in the coolant passages of regeneratively cooled nuclear rocket nozzles is to compare the calculations with experimental results.

The nozzle calculations were made using an existing digital computer program<sup>(7)</sup> which was revised to make use of these recommended equations for heat transfer and friction. Comparisons between predicted and measured gas-side wall temperature, coolant pressure drop, and coolant temperature rise are made for several NERVA nuclear tests. Wall temperatures were not measured in the Phoebus 2 and Pewee nuclear tests, so that only the measured coolant pressure drop and temperature rise were compared with predictions.

Pewee, NERVA, and Phoebus 2 vary a great deal in size and power but are in the same geometrical class of nozzles. These calculation procedures can and should be compared with experiments for other geometries when available.

## II. Basic Equations

### Coolant Side

Heat transfer. - Heat transfer coefficients in the coolant passages are calculated using the straight tube correlation equation<sup>(1)</sup> modified to include the effect of entrance configuration and curvature.<sup>(5)</sup>

The recommended straight tube correlation is

$$Nu_b = 0.023 Re_b^{0.8} Pr_b^{0.4} \left( \frac{T_w}{T_b} \right)^{-c_1} \quad (1)$$

where

$$c_1 = \left( 0.57 - \frac{1.59}{\frac{x}{D}} \right)$$

Eq. (1) modified to include entrance effects gives

$$Nu_b = 0.023 Re_b^{0.8} Pr_b^{0.4} \left( \frac{T_w}{T_b} \right)^{-c_1} \left( 1 + F_1 \frac{D}{x} \right) \quad (2)$$

where  $F = 2.3$  for a 45° angle bend and 5 for a 90° angle bend.

The  $I\bar{w}$  correction for the effects of curvature on friction coefficients<sup>(3)</sup> has been applied to local heat-transfer coefficients with good results<sup>(5)</sup> using Eq. (1) to give

$$Nu_b = 0.023 Re_b^{0.8} Pr_b^{0.4} \left( \frac{T_w}{T_b} \right)^{-c_1} \left[ Re_b \left( \frac{r}{R} \right)^2 \right]^{0.05} \quad (3)$$

for the concave side (throat) and

$$Nu_b = 0.023 Re_b^{0.8} Pr_b^{0.4} \left( \frac{T_w}{T_b} \right)^{-c_1} \left[ Re_b \left( \frac{r}{R} \right)^2 \right]^{-0.05} \quad (4)$$

for the convex side (knuckle).

Eqs. (1) to (4) cover all the conditions encountered in the cooling passages of nuclear rocket nozzles.

**Fluid flow.** - The range of conditions for which friction coefficients have been reported is not so great as those for heat-transfer coefficients. An investigation using all available data found that measured friction coefficients have been reported which were as much as three times the values predicted by conventional methods.<sup>(6)</sup> The correlation equation recommended

$$\frac{f}{2} = \left( 0.0007 + \frac{0.0625}{Re_w^{0.32}} \right) \left( \frac{T_w}{T_b} \right)^{-0.5} \quad (5)$$

where  $Re_w$  is the Reynolds number based on diameter and with viscosity and density evaluated at the wall temperature. This is the Koo, Drew, and McAdams relation modified with  $(T_w/T_b)^{-0.5}$ . For  $Re_w \geq 3000$  Eq. (5) correlated all the friction coefficients within  $\pm 10$  percent.

Eq. (5) can be used at  $x/D$  as low as 3 if the exponent of  $T_w/T_b$  is changed from 0.5 to the  $c_1$  used for heat transfer.

The Karman-Nikuradse relation can also be modified with  $(T_w/T_b)^{c_1}$  to give

$$\frac{1}{\sqrt{f}} = \left[ 4.0 \log (Re_w \sqrt{f}) - 0.40 \right] \left( \frac{T_w}{T_b} \right)^{c_1} \quad (6)$$

Assuming that the effect of  $T_w/T_b$  on the friction coefficient is the same for a rough tube as it is for a smooth tube, the equation for predicting friction coefficients in a rough tube<sup>(7)</sup> becomes

$$\frac{1}{\sqrt{f}} = \left[ -4.0 \log \left( \frac{e}{3.7 D} + \frac{1.255}{Re_w \sqrt{f}} \right) \right] \left( \frac{T_w}{T_b} \right)^{c_1} \quad (7)$$

where  $e$  is the relative roughness of the tube.

The  $160$  correction for the effect of curvature<sup>(3)</sup> should be used with both Eqs. (6) and (7). For friction coefficient calculations the exponent of

$$\left[ Re_w \left( \frac{r}{R} \right)^2 \right]$$

is 0.05 for both the throat and knuckle region because unlike the heat-transfer coefficient which is affected by only the heated surface the friction coefficient is affected by the wetted surface of the coolant passage. The heat-transfer coefficient would then decrease in the knuckle region while the friction coefficient would increase.

The  $160$  correction is used for both heat transfer and friction even though it was originally proposed for only friction. How well the  $160$  correction applies to local heat transfer and friction has not been studied thoroughly due to the paucity of local experimental data reported for both heat transfer and friction coefficients.

The friction pressure drop is calculated from

$$\Delta p_{fr} = \frac{2G^2 f x}{Dg} \quad (8)$$

The momentum pressure drop is calculated from

$$\Delta p_{mom} = \frac{w^2}{gA} \left[ \frac{1}{(\rho A)_2} - \frac{1}{(\rho A)_1} \right] \quad (9)$$

The total pressure drop is the sum of the friction and momentum pressure drops.

#### Hot-Gas Side

In calculating the heat transfer from the hot gas to the cooled nozzle wall, it is common practice to use the Nusselt equation

$$Nu_f = C_g Re_f^{0.8} Pr_f^{0.4} \quad (10)$$

and vary the  $C_g$  as a function of axial location or area ratio. The value of  $C_g$  can either be measured<sup>(8)</sup> or calculated, e.g. Bartz boundary layer calculations.<sup>(9)</sup> These  $C_g$  values are usually adjusted after rocket tests to give calculated gas-side wall temperatures equal to measured values. In cooled nozzles the  $C_g$  thus becomes a function of coolant side heat transfer equations. The theoretical values of  $C_g$  calculated by the Aerojet General Corp. for NERVA and Phoebus 2 nuclear runs are shown in Fig. 1.

The value of  $C_g$  increases in the nozzle chamber from knuckle to reactor core face but the area ratio remains constant which is indicated by the vertical line in Fig. 1(a). The area ratio of the nozzle chamber is not the same for NERVA, Phoebus 2, and Pewee.

Figure 1(b) shows the theoretical and adjusted  $C_g$  curves for the NERVA nozzle. The adjusted value of  $C_g$  is about 2.5 times the theoretical value in the knuckle region. The need for such a high  $C_g$  in this region probably results from the lack of previous coolant side correlation equations to take into account

the decrease in heat-transfer due to the convex curvature. This effect of curvature appears in Eq. (4). The  $C_g$  values shown for the Pewee nozzle were experimentally determined by Los Alamos Scientific Laboratory. The data points were reported by Schacht, Quentmeyer, and Jones.<sup>(8)</sup>

In Eq. (10) the Reynolds number is based on nozzle diameter. It would be more logical to treat the constant diameter chamber section as a flat plate and base the Reynolds number on axial distance along the wall were it not for the introduction of cold hydrogen for peripheral film cooling of that section.

### III. Nozzle Calculations

The nozzle calculations were made using the digital computer program of Rohde, Duscha, and Derderian<sup>(7)</sup> modified to incorporate the equations recommended in this paper.

#### Coolant Side

**Heat transfer.** - A Nusselt type correlation equation with the physical properties evaluated at the film temperature is part of the computer program.<sup>(7)</sup> This equation was replaced by Eq. (1) with the effects of entrance configuration and curvature being applied in the proper regions as shown in Fig. 2.

**Fluid flow.** - The friction coefficients are calculated in the program using the Karman-Nikuradse relation for smooth tubes and the rough tube equation which was modified to become Eq. (7). The relative roughness  $e$ , of the coolant passages is as follows: NERVA:  $e = 5 \mu\text{in.}$ , Phoebus 2:  $e = 10 \mu\text{in.}$ , Pewee:  $e = 20 \mu\text{in.}$ , and Eq. (7) was used in the nozzle calculations as shown in Fig. 2.

The surface temperature of the coolant passage varies as much as  $1000^\circ\text{R}$  from the crown (the semi-circular portion of the U-tube) to the pressure shell (see Fig. 3). This temperature variation makes the calculation of a single friction coefficient for the complete wetted perimeter very difficult. Calculations of pressure drop through the coolant passages are often 60 percent lower than the measured drop. The following results indicate the variation in friction coefficients which can result from two different assumptions for a section of coolant passage well downstream of the entrance region and upstream of the throat curvature in the NERVA nozzle using Eq. (7).

**Assumption 1** - The cooling passage wall temperature is constant and equal to the hydrogen bulk temperature  $T_w = T_b$ .  $T_w/T_b = 1$ ,  $Re_w = Re_b = 2.7 \times 10^7$ ,  $f = 0.00267$ .

**Assumption 2** - The cooling passage wall temperature is constant and equal the crown temperature.  $T_w = 1200^\circ\text{R}$ ,  $T_b = 80^\circ\text{R}$ ,  $T_w/T_b = 15$ ,  $Re_w = 8.9 \times 10^4$ ,  $f = 0.0009$ .

There is a factor of 3 between the two friction coefficients.

The method used herein was to calculate one friction coefficient for the bulk temperature ( $f_b$ ) and another for the hot crown temperature ( $f_c$ ) for each station. Then an effective friction coefficient was defined as

$$f_{\text{eff}} = f_b \left( \frac{S_b}{S_b + S_c} \right) + f_c \left( \frac{S_c}{S_b + S_c} \right) \quad (11)$$

where  $f_{\text{eff}}$  is the effective friction coefficient,  $S_b$  and  $S_c$  are the surface areas at bulk and crown temperatures respectively as shown in Fig. 3.

Values of  $(S_c/S_b + S_c)$  and  $(S_b/S_b + S_c)$  were calculated at each calculation station along the coolant passage and  $(S_c/S_b + S_c)$  varied from 0.40 at the coolant entrance to 0.22 at the nozzle throat and 0.60 in the chamber of the NERVA nozzle.

Eq. (11) should be as applicable to a rectangular (or any other shape) coolant passage as to the U-tube passage.

The momentum pressure drop equation in the computer program<sup>(7)</sup> remained unchanged.

#### Hot-Gas Side

The heat transfer coefficients on the hot gas side were calculated with the Nusselt type equation in the original program.<sup>(7)</sup> The values for  $C_g$  are input data and therefore the effects of the various  $C_g$ 's can be observed.

Hot gas static temperature and pressure calculations for hydrogen at equilibrium conditions for assigned chamber pressure, chamber temperature, and nozzle area ratios were made using the computer program of Ref. 10.

The effect of peripheral film cooling in the chamber was calculated using the method of Hatch and Papell.<sup>(11)</sup> In the NERVA and Phoebus 2 nozzles the film coolant temperature was about  $1200^\circ\text{R}$  and the flow rate was about 1 percent of the hot gas flow rate. The coolant was assumed to effect the coolant passage wall temperature for a distance of 6 in. from the reactor core. The Pewee nozzle had a coolant flow rate of about 10 percent of the hot gas flow rate and a temperature as low as  $200^\circ\text{R}$ . For the Pewee calculations the coolant was assumed to have some effect all the way to the knuckle region.

### IV. Discussion of Results

The only experimental wall temperatures available from nuclear tests are for the NERVA nozzles NRX-A3, EST, A5, and A6. Coolant pressure drop and temperature rise were also measured for these tests as well as the peripheral coolant temperatures and flow rates. This information made the NRX series suitable for the test of the modified computer program.

Gas-side wall temperatures predicted using the AGC theoretical  $C_g$ , the AGC adjusted  $C_g$ , and a constant  $C_g$  of 0.026 are compared to experimental gas-side wall temperatures for NRX-A6 in Fig. 4. The experimental wall temperatures resulted from an examination of braze alloy patches at various locations in the nozzle. The open and solid symbols are at different angular locations ( $105^\circ$  apart) in the nozzle. The solid lines represent the wall temperatures calculated with and without film cooling using the theoretical values of  $C_g$  for the NERVA nozzle geometry and is in very good agreement with the measured values for most of the length. The wall temperatures calculated with and without film cooling using the adjusted values of  $C_g$  were much higher than the measured wall temperatures in the chamber and knuckle regions. These higher calculated wall temperatures resulted from a combination of high values of  $C_g$  in the adjusted curve (see Fig. 1(b)) and a decrease in the coolant heat-transfer coefficient due to the convex curvature effect in Eq. (4). It appears that the effect of convex curvature has been included twice, once on the heat-gas side and once on the coolant side.

It is very difficult to compare the predicted and measured wall temperatures near the core because the cold hydrogen used for peripheral film cooling is introduced at this point. Predicted wall temperatures are shown with and without peripheral film cooling. Experimental studies have shown that the inclusion of a simulated reactor core can increase the heat-transfer coefficients in a nozzle chamber.<sup>(12)</sup>

The dashed line in Fig. 4 represents the wall temperature calculated using a constant  $C_g$  of 0.026, the simplified method represents the wall temperatures fairly well. The predicted wall temperatures near the core were lower than the measured temperatures even though film cooling (the film coolant temperature is about  $500^\circ\text{R}$  higher than the wall temperature) was not included in these calculations. However, in a nozzle without peripheral film cooling, the use of a constant  $C_g$  would predict wall temperatures which could be much lower than the actual temperatures near the reactor core.

For the NRX-A6 test the pressure drop calculated using Eq. (11) was 139 psi compared to the measured value of 141 psi. The calculated temperature rise is  $95^\circ\text{R}$  which is a good agreement with the measured rise of  $93^\circ\text{R}$ . If the coolant passage wall temperature is assumed to be constant and equal to the bulk temperature, the calculated pressure drop is 153 psi, about 8.5 percent higher than the measured value and still in good agreement with measured values. The pressure drop and temperature rise for the various NRX test nozzles are shown in Table 1. The variation of coolant temperature and pressure along the length of the nozzle is shown in Fig. 5.

The computer program was also used to calculate wall temperatures and coolant conditions for the Pewee and Phoebus-2 nuclear tests. The coolant pressure drop and temperature rise for Phoebus 2 and Pewee tests are also shown in Table 1.

For the Pewee nozzle the agreement between calculated and measured temperatures rise and pressure drop was usually better for the full power tests than for other tests.

The film coolant flow rate was about 10 percent of the hot gas flow rate for the Pewee nozzle compared to about 1 percent for NERVA and Phoebus 2 nozzles. In addition the coolant temperature was much lower for Pewee than for NERVA and Phoebus 2. These facts might tend to lower the confidence level for any Pewee wall temperature calculations to some degree.

The fact that calculated pressure drops are in almost all tests about 10 percent lower than the measured value indicates that possibly the method of weighting the friction coefficients on the surface area with which it is in contact over corrects the effective coefficients in Eq. (11). Another possibility is that the effect of wall to bulk temperature ratio which has been verified for smooth tubes with temperature ratios up to 7.35 cannot be extrapolated to rough passages with temperature ratios of 15.

## V. Conclusions

It appears from the results of this study that the use of the best available prediction equations for heat transfer and friction coefficients for turbulent flow through tubes can, with modifications for entrance and curvature effects, be applied with good results to the coolant passages of nuclear rocket nozzles. These equations should also be useful for any type of rocket nozzle in this geometry class.

It should be concluded from the results presented in this paper that existing variable property heat transfer and friction equations can be used to predict coolant pressure and temperatures and nozzle wall temperatures with reasonable accuracy. These results form a basis with which future calculational methods can be compared, and hopefully improved.

## VI. Symbols

A	cross-sectional area
$C_g$	coefficient in heat-transfer equation
$c_1$	exponent of $T_w/T_b$
D	diameter
e	relative roughness of surface
F	entrance effect coefficient
f	friction coefficient
G	mass flow rate per unit cross-sectional area
g	gravitational conversion factor
Nu	Nusselt number

Pr	Prandtl number
$\Delta p$	total static pressure drop
$\Delta p_{fr}$	friction pressure drop
$\Delta p_{mom}$	momentum pressure drop
R	radius of curvature
Re	Reynolds number
r	inside radius of passage
S	surface area
T	temperature
w	mass weight of flow
x	linear distance from entrance
$\rho$	density

#### Subscripts:

b	bulk
c	crown
g	gas
w	wall

### VII. References

1. Taylor, M. F., "Correlation of Local Heat Transfer Coefficients for Single Phase Turbulent Flow of Hydrogen in Tubes with Temperature Ratios to 23," TN D-4332, 1968, NASA, Cleveland, Ohio.
2. Anon., "Heat Transfer to Cryogenic Hydrogen Flowing Turbulently in Straight and Curved Tubes at High Heat Fluxes," CR-678, 1967, NASA, Washington, D.C.
3. Itō, H., "Friction Factors for Turbulent Flow in Curved Pipes," Journal of Basic Engineering, Vol. 81, No. 2, June 1959, pp. 123-134.
4. Stinnett, W. D., "An Experimental Investigation of the Heat Transfer to Hydrogen at Near Critical Temperatures and Supercritical Pressures Flowing Turbulently in Straight and Curved Tubes," Rept. 2551, NASA CR-50836, May 1963, Aerojet-General Corp., Azusa, Calif.
5. Taylor, M. F., "Heat-Transfer Predictions in the Cooling Passages of Nuclear Rocket Nozzles," Journal of Spacecraft and Rockets, Vol. 5, No. 11, Nov. 1968, pp. 1353-1355.
6. Taylor, M. F., "Correlation of Friction Coefficients for Laminar and Turbulent Flow with Ratios of Surface to Bulk Temperature from 0.35 to 7.35," TR R-267, 1967, NASA, Cleveland, Ohio.
7. Rohde, J. E., Duscha, R. A., and Derderian, G., "Digital Codes for Design and Evaluation of Convectively Cooled Rocket Nozzle with Application to Nuclear-Type Rocket," TN D-3798, 1967, NASA, Cleveland, Ohio.
8. Schacht, R. L., Quentmeyer, R. J., and Jones, W. L., "Experimental Investigation of Hot-Gas Side Heat-Transfer Rates for a Hydrogen-Oxygen Rocket," TN D-2832, 1965, NASA, Cleveland, Ohio.
9. Ellicott, D. G., Bartz, D. R., and Silver, S., "Calculation of Turbulent Boundary-Layer Growth and Heat Transfer in Axi-Symmetric Nozzles," JPL-TR-32-387, Feb. 1963, Jet Propulsion Lab., California Inst. Tech., Pasadena, Calif.
10. Gordon, S., Zeleznik, F. J., and Huff, V. N., "A General Method for Automatic Computation of Equilibrium Compositions and Theoretical Rocket Performance of Propellants," TN D-132, 1959, NASA, Cleveland, Ohio.
11. Hatch, J. E. and Papell, S. S., "Use of a Theoretical Flow Model to Correlate Data for Film Cooling or Heating an Adiabatic Wall by Tangential Injection of Gases of Different Fluid Properties," TN D-130, 1959, NASA, Cleveland, Ohio.
12. Schmidt, J. F., Boldman, D. R., Ehlers, R. C., and Coats, J. W., "Experimental Study of Effect of Simulated Reactor Core Position on Nozzle Heat Transfer," TM X-1208, 1966, NASA, Cleveland, Ohio.

TABLE 1 CALCULATED AND MEASURED TEMPERATURE RISE AND PRESSURE DROP ACROSS COOLANT PASSAGES FOR NUCLEAR TESTS

NERVA

Nozzle	Pressure drop			Temperature rise		
	Calculated $\Delta p_c$ , psi	Measured $\Delta p_m$ , psi	$\frac{\Delta p_c - \Delta p_m}{\Delta p_m} \times 100$ , percent	Calculated $\Delta T_c$ , °R	Measured $\Delta T_m$ , °R	$\frac{\Delta T_c - \Delta T_m}{\Delta T_m} \times 100$ , percent
NRX-A3	137	134	2.2	87	89	-2.2
NRX-A4	153	179	-14.5	90	88	2.3
NRX-A5	144	141	2.1	94	103	-8.7
NRX-A6	139	141	-1.4	95	93	2.1

Phoebus-2

EP-IV Anointed time	Pressure drop			Temperature rise	
	Calculated $\Delta p_c$ , psi	Measured $\Delta p_m$ , psi	$\frac{\Delta p_c - \Delta p_m}{\Delta p_m} \times 100$ , percent	Calculated $\Delta T_c$ , °R	Range of measured $\Delta T_m$ , °R
1	27	29	-6.9	26	13 to 36
2	60	66	-9.1	31	28 to 41
3	132	151	-12.6	55	38 to 62
4	182	204	-10.8	52	33 to 60
5	211	255	-17.3	78	57 to 88
6	246	290	-15.2	83	60 to 93

Pewee

EP III	Pressure drop			Temperature rise		
	Calculated $\Delta p_c$ , psi	Measured $\Delta p_m$ , psi	$\frac{\Delta p_c - \Delta p_m}{\Delta p_m} \times 100$ , percent	Calculated $\Delta T_c$ , °R	Measured $\Delta T_m$ , °R	$\frac{\Delta T_c - \Delta T_m}{\Delta T_m} \times 100$ , percent
37	59	62	-4.8	62	56	10.7
FP1A	117	126	-7.1	94	91	3.3
B	108	118	-8.5	93	92	1.1
C	113	124	-8.9	94	93	1.1
D	113	124	-8.9	94	93	1.1
341	31	37	-16.2	23	24	-4.2
FP2A	113	123	-8.1	94	93	1.1
B	113	125	-9.6	94	96	-2.1
C	113	125	-9.6	94	96	-2.1
D	113	125	-9.6	94	97	-3.1
342	31	37	-16.2	23	25	-8.0



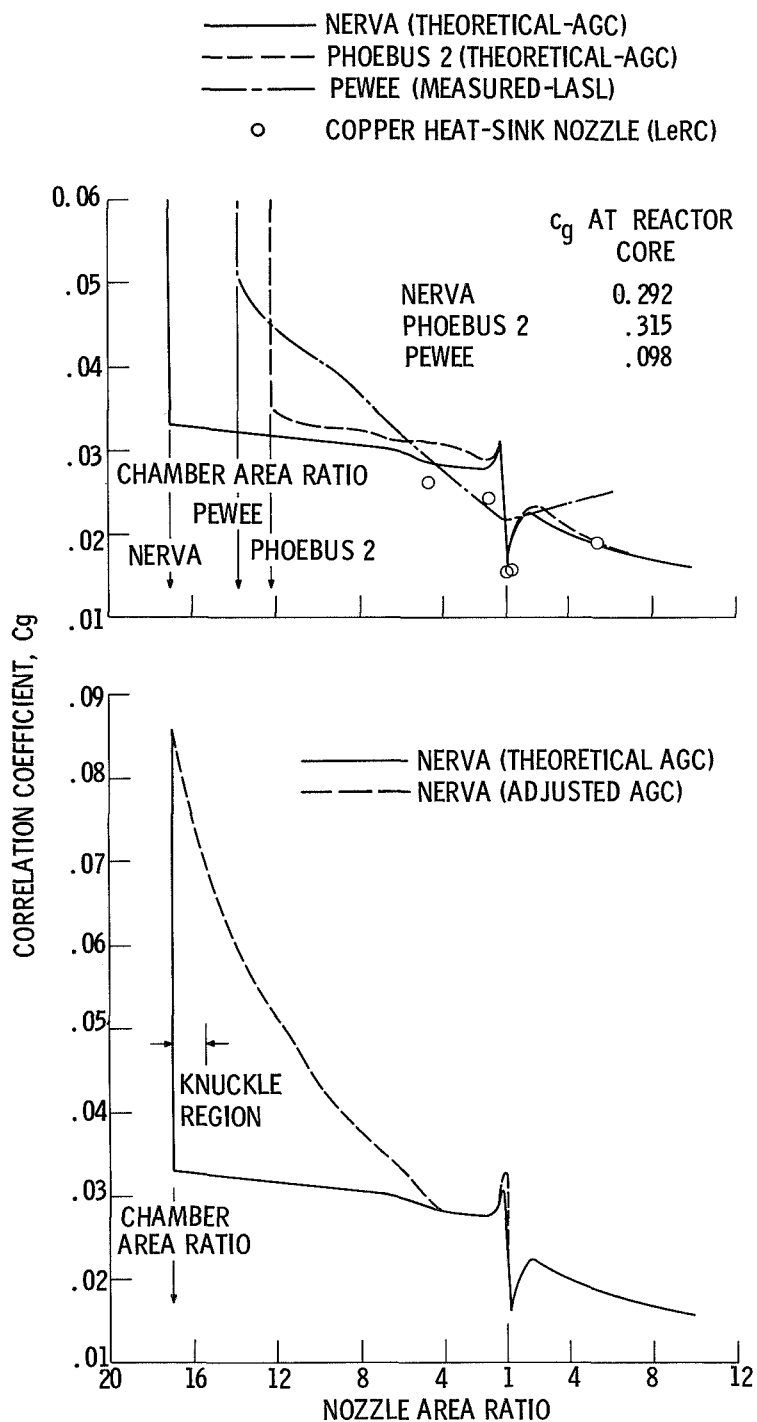
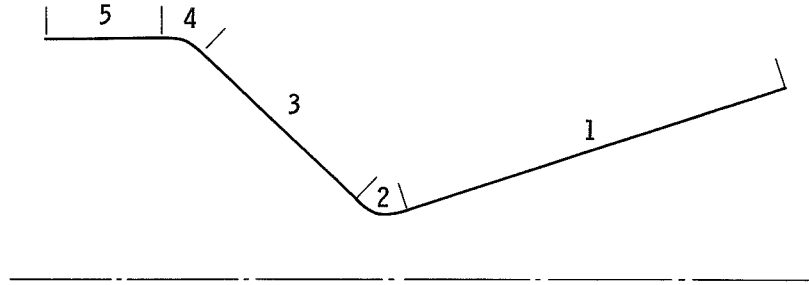


Figure 1. - Variation of various correlation coefficients for hot-gas side heat transfer as a function of area ratio.



Region	Heat transfer	Friction
1	$Nu_b = 0.023 Re_b^{0.8} Pr_b^{0.4} \left( \frac{T_w}{T_b} \right)^{-c_1} \left( 1 + F_1 \frac{D}{x} \right)$	$\frac{1}{\sqrt{f}} = \left[ -4.0 \log \left( \frac{e}{3.7 D} + \frac{1.255}{Re_w \sqrt{f}} \right) \right] \left( \frac{T_w}{T_b} \right)^{c_1}$
2	$Nu_b = 0.023 Re_b^{0.8} Pr_b^{0.4} \left( \frac{T_w}{T_b} \right)^{-c_1} \left[ Re_b \left( \frac{r}{R} \right)^2 \right]^{0.05}$	$\frac{1}{\sqrt{f}} = \left[ -4.0 \log \left( \frac{e}{3.7 D} + \frac{1.255}{Re_w \sqrt{f}} \right) \right] \left( \frac{T_w}{T_b} \right)^{c_1} \left[ Re \left( \frac{r}{R} \right)^2 \right]^{-0.05}$
3	$Nu_b = 0.023 Re_b^{0.8} Pr_b^{0.4} \left( \frac{T_w}{T_b} \right)^{-c_1}$	$\frac{1}{\sqrt{f}} = \left[ -4.0 \log \left( \frac{e}{3.7 D} + \frac{1.255}{Re_w \sqrt{f}} \right) \right] \left( \frac{T_w}{T_b} \right)^{c_1}$
4	$Nu_b = 0.023 Re_b^{0.8} Pr_b^{0.4} \left( \frac{T_w}{T_b} \right)^{-c_1} \left[ Re_b \left( \frac{r}{R} \right)^2 \right]^{-0.05}$	$\frac{1}{\sqrt{f}} = \left[ -4.0 \log \left( \frac{e}{3.7 D} + \frac{1.255}{Re_w \sqrt{f}} \right) \right] \left( \frac{T_w}{T_b} \right)^{c_1} \left[ Re \left( \frac{r}{R} \right)^2 \right]^{-0.05}$
5	$Nu_b = 0.023 Re_b^{0.8} Pr_b^{0.4} \left( \frac{T_w}{T_b} \right)^{-c_1}$	$\frac{1}{\sqrt{f}} = \left[ -4.0 \log \left( \frac{e}{3.7 D} + \frac{1.255}{Re_w \sqrt{f}} \right) \right] \left( \frac{T_w}{T_b} \right)^{c_1}$

Figure 2. - Five regions of the coolant passage and equations applicable to each region.

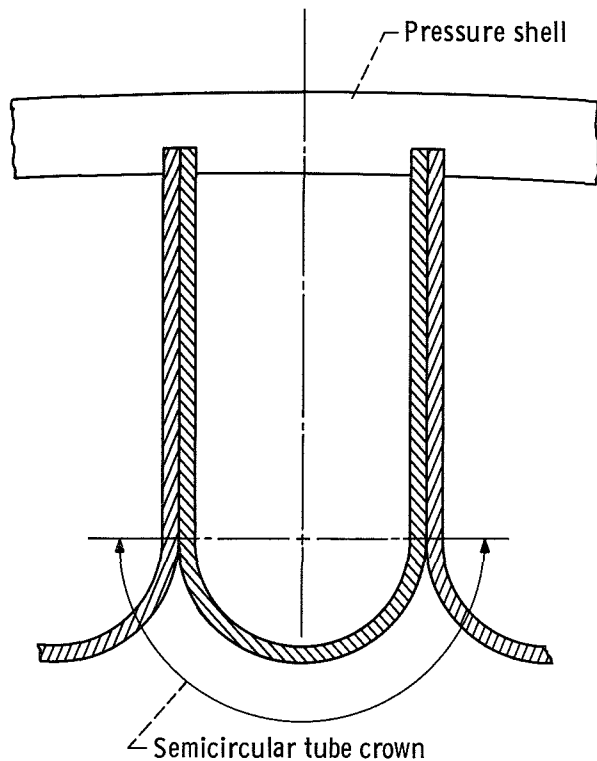


Figure 3. - Typical U-tube coolant passage of a nuclear rocket nozzle.

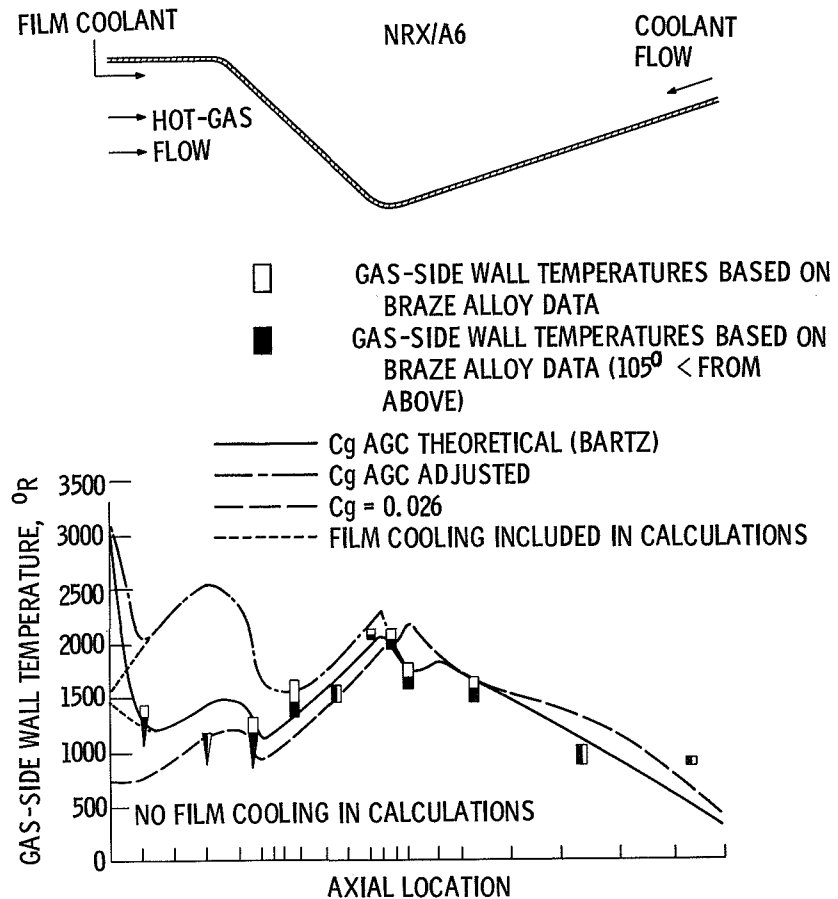


Figure 4. - Comparison of calculated gas-side wall temperatures with measured values for NRX-A6 nuclear test, NERVA nozzle.

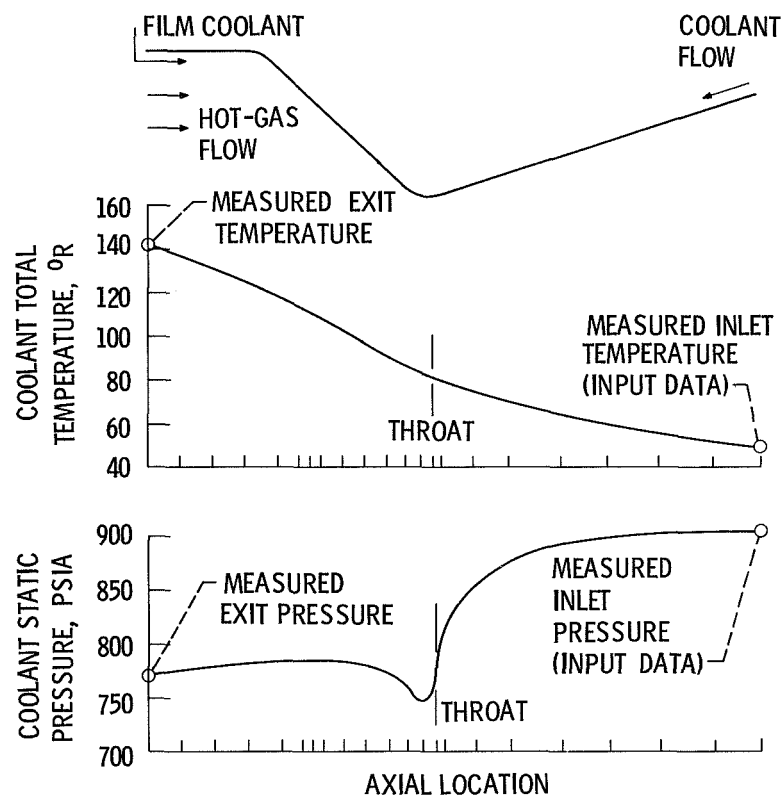


Figure 5. - Variation of coolant temperature and pressure with axial location. NRX-A6 nuclear test, NERVA nozzle.